Fault structure and biogenic soil calcite near Ivanpah Spring, Clark Mountain, San Bernardino County, California

David K. Lynch[1], Paul M. Adams[2], and David S. P. Dearborn[3]
[1]Thule Scientific, corresponding author, david@alumni.caltech.edu; [2]Thule Scientific; [3]Lawrence Livermore National Laboratory

ABSTRACT: Based on offset channels, soil color and vegetation lineaments along its approximately 2.5 km surface exposure, the Ivanpah Spring Fault appears to be a right lateral transform fault striking ~N45W. It shows a right-hand bend or step-over (releasing bend) near Ivanpah Spring with an offset of about 50 m. Direct surveying and topographic maps derived by stereo imagery reveals an indentation in the elevation profile through the step-over region. It appears to be a small, sag-like transtensional pull-apart that is ~35 m across and ~2 m deep. The "sag," however, does not collect standing water because it is on a slope and has no elevation minimum. The lowest part of the sag has dark brown soil and also has the lowest slope in the transect, nearly horizontal. Surface run off would flow slower here than in steeper parts and the sag would tend to absorb more runoff water. This may explain the enhanced vegetation in the sag, which attracts herbivores, mainly cows and burros. Field inspection, photomicrography, X-ray diffraction (XRD), infrared spectroscopy (IRS), energy dispersive X-ray spectroscopy (EDS), and thermogravimetric Analysis (TGA) of soils along the transect through the sag reveal that the dark soil is due to relatively large amounts of dung (and by association urine) with elevated amounts of $CaCO_3$. There is a strong correlation between organic material (C-H) and pedogenic $CaCO_3$. We suggest that the $CaCO_3$ originates primarily from herbivore urine, though some of it may be the result of biomineralization by urealytic bacteria acting on decomposing dung through microbiologically induced calcite deposition (MICD).

1. Introduction

Ivanpah Spring (35.540303 -115.529610) is man-modified seep[1] in a former gold and silver mining area[2] on the southeast flank of Clark Mountain (Figure 1) in San Bernardino County (Ivanpah Quadrangle). The country rock is primarily a Precambrian metamorphic complex of foliated gneissic with alkali feldspar igneous intrusions and dikes[3-5]. Springs are often associated with faults[6] and the Ivanpah Spring Fault passes through or near the spring. The fault was identified and mapped from aerial photographs and field inspection. In this paper we (1) report field observations of fault structures near the spring and (2) present evidence for biologically induced pedogenic $CaCO_3$ in a dung-rich sag-like feature.

2. Surveying the fault

We visited the site several times during 2017, and the fault trace was visually inspected on foot along its ~2.5 km long surface exposure. Particular attention was paid to a small region located ~50 m WSW of the spring with uncharacteristically dark brown soil and showed unusual slope changes, vegetation enhancements and scattered groundwater discharge deposits. Using a handheld Garmin 60CSx receiver, we measured vertical profiles of transects that ran more or less along the line of

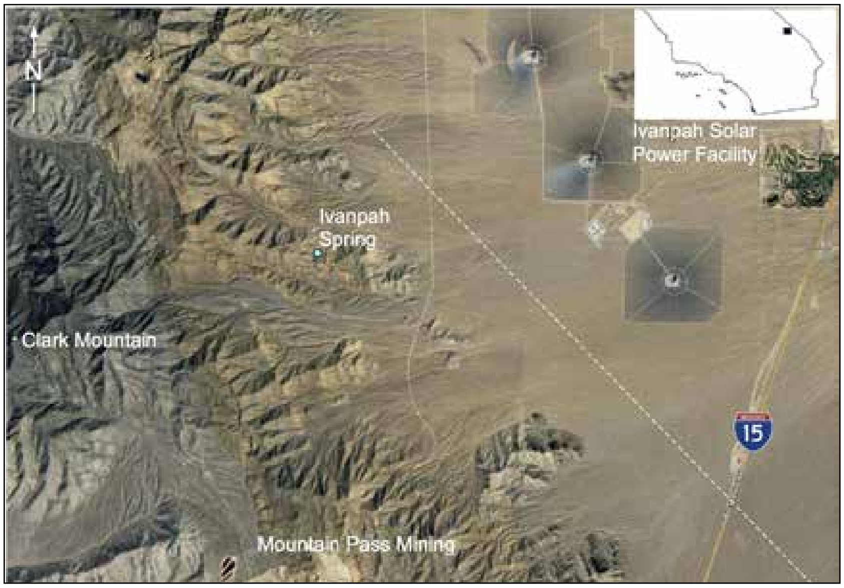

Figure 1. Annotated Google Earth map of the Ivanpah Spring area. The Clark Mountain Fault system is evident to the left as two ~N30E striking lineaments. The white dashed line is the approximate location of the putative Ivanpah Fault based on Wilkerson's map[5].

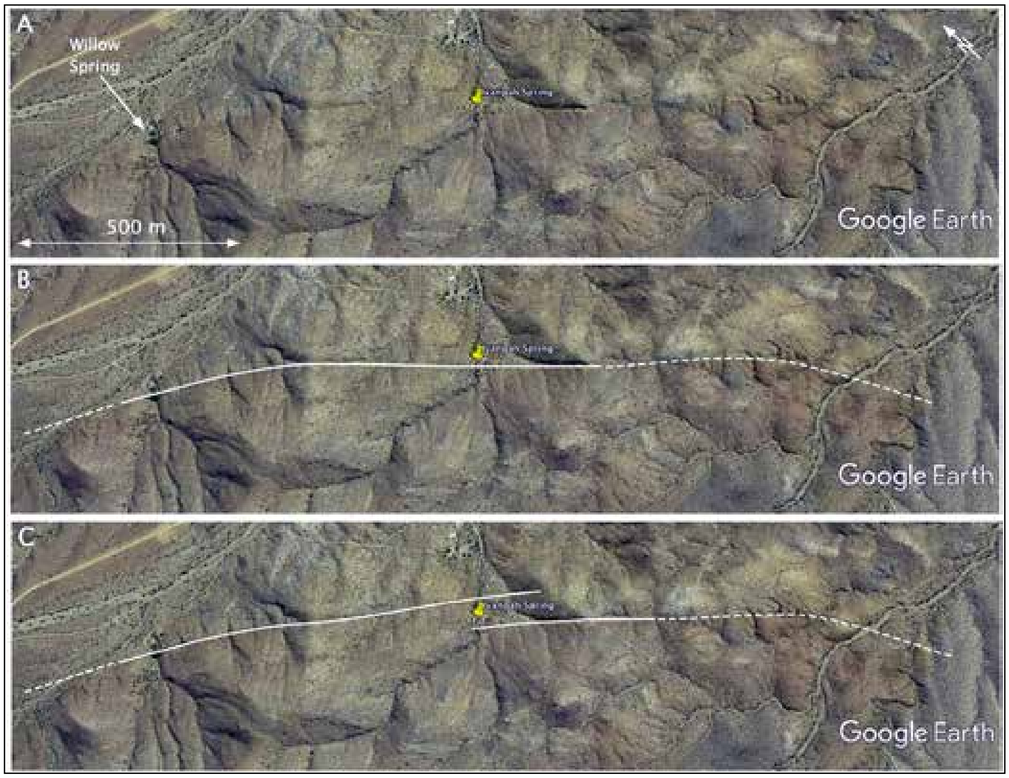

Figure 2. (A) Google Earth image showing the location of Ivanpah Spring (yellow pushpin at the center of image). (B) Fault trace based on offset streams and soil color boundaries. (C) Fault trace when vegetation enhancements and unusual topography are included.

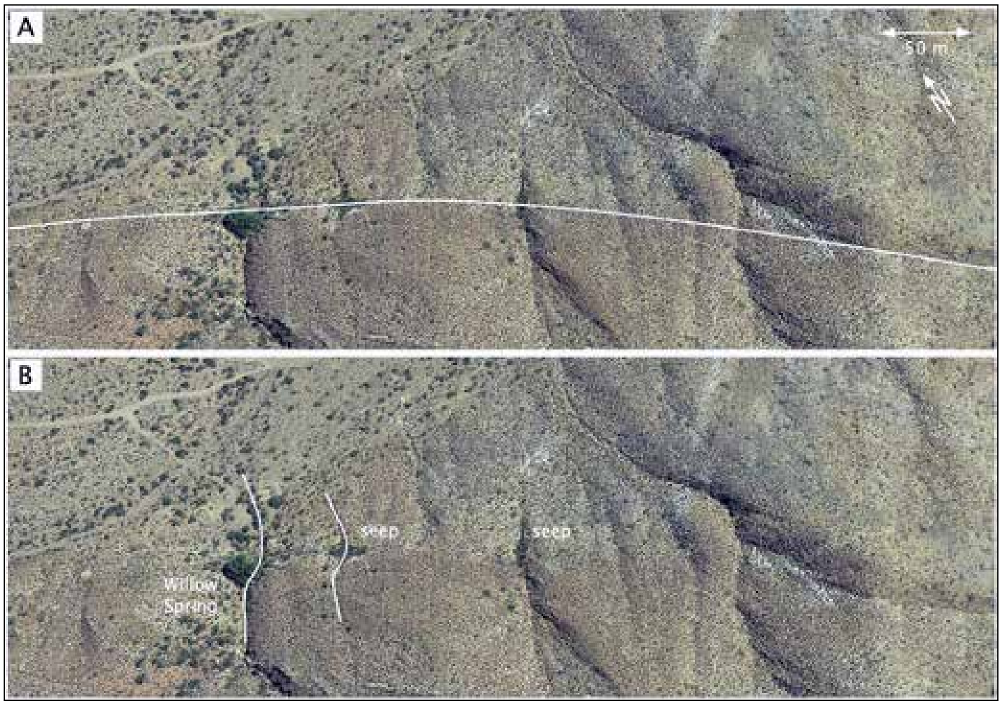

Figure 3. Two stream channels show apparent right lateral offset along the fault. (A) The white line shows the inferred fault trace. (B) Two white curved lines mark channel offset of Willow Spring and an unnamed seep.

steepest decent starting and ending in areas with typical vegetation and soil colors and passing through the brown area. The transects were nearly perpendicular to the strike of the fault. Elevation was measured approximately every 15 meters along the transects' 110 m lengths. Soil samples were collected at six locations, two of them in the area of brown soil.

After placing seven control point markers around the area, we took stereo pictures of the site separated by 75 m from a nearby hill that was about 23 meters above the brown area and 110 meters from it. The stereo images were later processed[7] to produce a digital surface model of elevations and contour map of the area, from which independent measurements of the transect profile were extracted.

3. Faults properties

Figure 2 shows a Google Earth photograph of the fault region as far as the fault can be visually followed. Figure 2A is presented with no interpretation. Figures 2B and 2C show two possible interpretations of the trace. The northwestern portion of the fault is well marked by offset stream channels, vegetation lineaments, soil color boundaries, linear gullies, and ridge notches (topographic saddles). Our original interpretation was that the fault passed through Ivanpah Spring. Further examination of the local topography suggested that there might be a bend or step over in the vicinity of the spring. Being on an elevated tongue of land, the curvature of the fault as seen in map view suggests that it is steeply dipping, possibly to the southwest. Mapped features highlighted on Figure 3 suggest that the sense of slip includes a right-lateral component. Channels associated with Willow Spring and an unnamed seep both showed apparent right-hand channel offset and enhanced vegetation consistent with a subsurface barrier to groundwater flow.

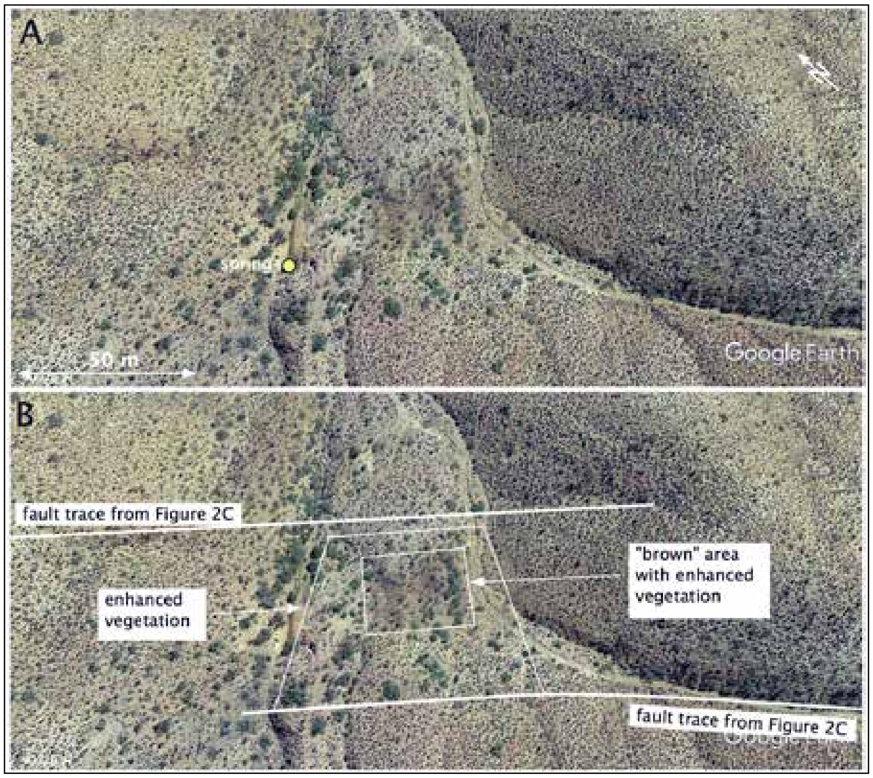

Figure 4. Step Over Region. A: Google Earth Image showing the location of Ivanpah Spring. B: Annotated Google Earth Image show the two inferred traces of the Ivanpah Spring Fault in the step over region based on field observations and Figure 2C.

4. Survey Results

A right hand step in a right lateral transform fault should produce a pull-apart basin (sag) and we found topography consistent with geometric complexity of this type. The topographic depression is roughly rectangular (35 x 40 m) and shows a number of features that differed markedly from its surroundings (Figure 4). It contains a high concentration of visibly abundant animal dung (hence the color) that correlated with noticeably enhanced vegetation density. Soil color, composition and vegetation density outside the enhanced vegetation area is typical of the larger area. The lowest part of the brown area is nearly horizontal, in contrast to the overall ~7° slope of the region. We marked off a transect approximately 110 m long that ran downhill and through the depressed brown area. While walking along the transect, it was obvious that the

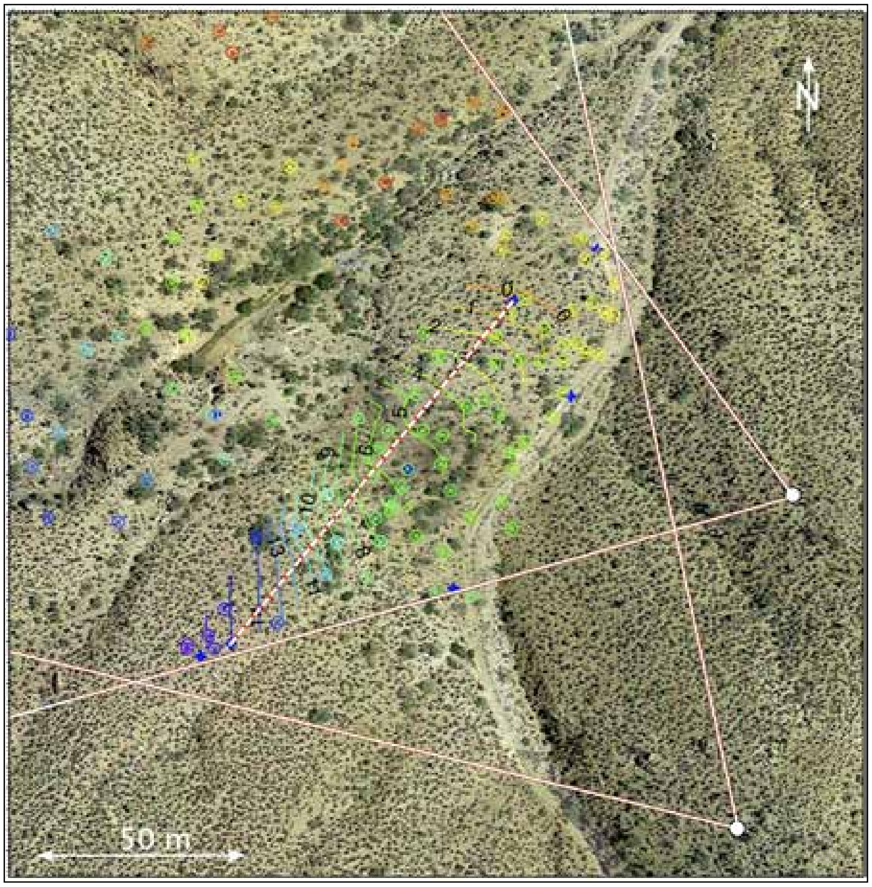

Figure 5. Annotated Google Earth image of the topographic depression of interest overlaid with the derived elevation contours along the transect (dashed line). White dots are the camera locations for the stereo pair and the white lines attached to the dots show the field of view of each camera image. The contours are at 1-meter vertical elevation intervals. The stars are gps surveyed control points used to orient the cameras resulting in a defined altitude and azimuth for each pixel. Triangulated points are shown as circles with a cross. The colors vary with elevation (See PDF version of the paper in the 2018 proceedings volume at www.desertsymposium.org). The contours were generated by interpolation among these points in the area of interest within about twenty meters of the transect).

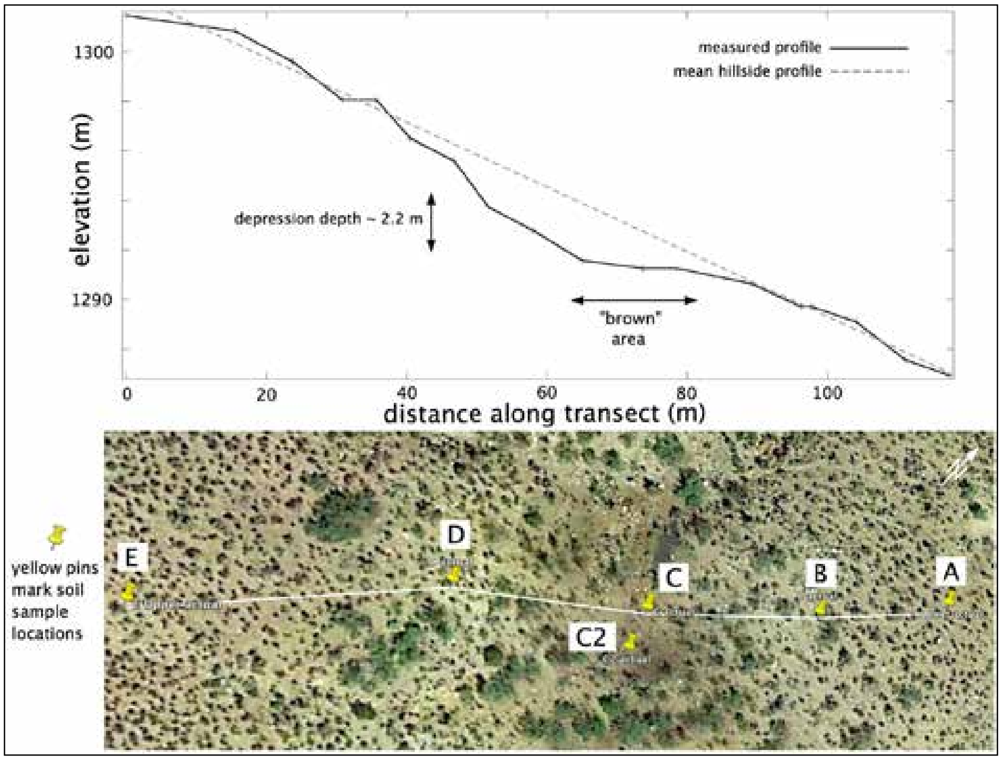

Figure 6. Upper: Transect profile. Lower: Google earth image with transect and soil sample locations. The smallest slope occurs in the brown area. C2 is about a meter lower than C.

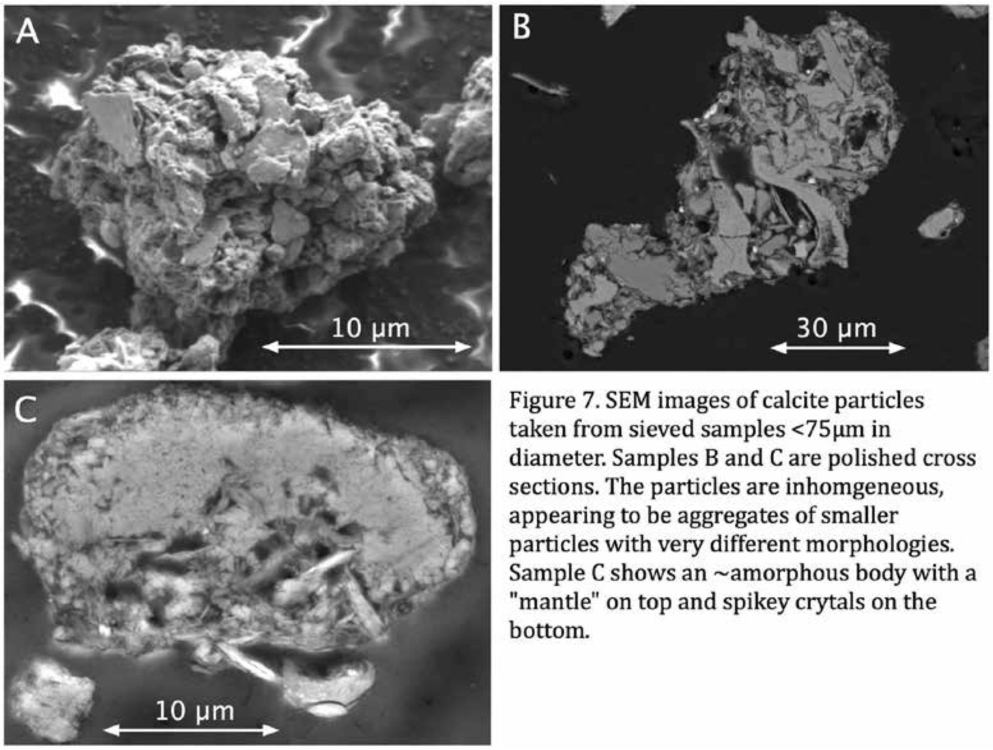

Figure 7. SEM images of calcite particles taken from sieved samples <75µm in diameter. Samples B and C are polished cross sections. The particles are inhomgeneous, appearing to be aggregates of smaller particles with very different morphologies. Sample C shows an ~amorphous body with a "mantle" on top and spikey crytals on the bottom.

slope was monotonic, i.e., at no point did it contain a local elevation minimum.

Elevation profiles of the transect were obtained three ways: (1) Google Earth topography, (2) walking the transect and marking positions with the Garmin, and (3) extracting profiles from a contour map produced from stereo imagery. All were consistent with one another.

Figure 5 shows the contour map and Figure 6 shows the profile obtained by averaging Garmin profiles.

The transect profile shows a depression about 50 m wide and 2.2 meters deep compared to the mean slope of the hillside. At its lower end the slope is small, almost horizontal but still with the same sign and the mean slope. At no place along the profile is there a minimum.

5. Soil Analysis

The purpose of analyzing the soil was to identify and map the composition, grain size and morphology of soil particles as a function of position along the transect. Surface soil samples were taken at six points along the transect (Figure 6) and sieved into three size groups: > 850 µm, 850 µm - 75 µm and <75 µm fractions, the latter of which were used for subsequent analyses. In samples C and C2 (and to lesser extent D) small seed husks and other plant debris were more common in the 850 µm - 75 µm fraction. X-ray diffraction (XRD) θ–2θ scans were performed with copper radiation using a PANalytical X'Pert Pro diffractometer equipped with an X'celerator strip detector.

Fourier transform infrared (FTIR) measurements were made with a Nicolet model 6700 spectrometer. Diffuse reflectance spectra were recorded with a Harrick Scientific Praying Mantis accessory using Labsphere Infragold as a background. Pseudo-transmission scans were performed with a Durascope single-bounce diamond attenuated total reflectance (ATR) accessory.

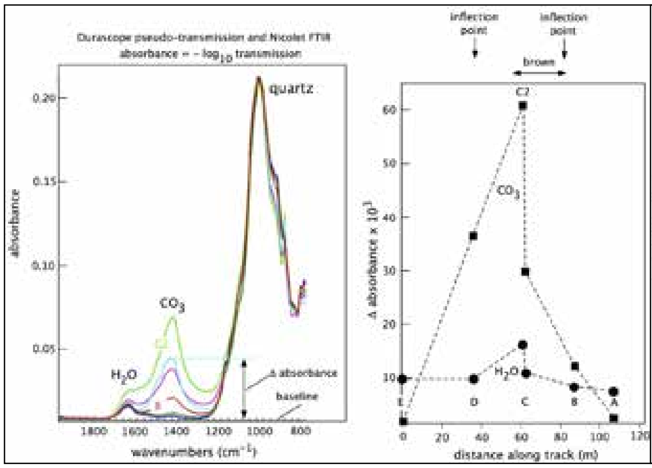

Figure 8. Left: Baseline corrected ATR reflectance FTIR spectra of the soil samples. Right: Relative signal strength of water and calcite along the transect. The upper end of the transect is at E and the lower end at A.

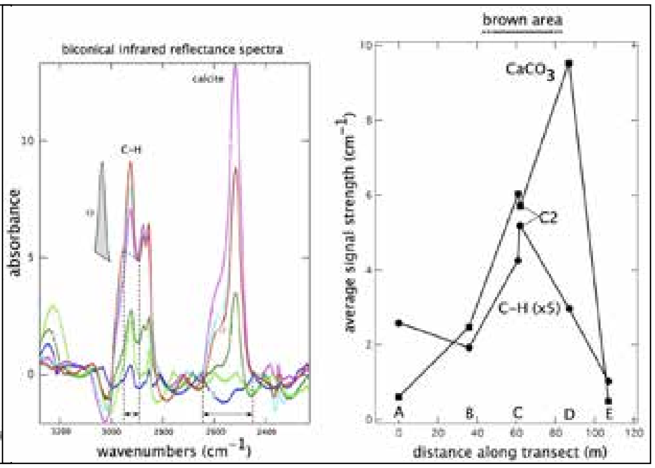

Figure 9. Left: Baseline corrected diffuse reflectance FTIR spectra of soil samples. The area of the C-H feature was measured between 2900 and 2952 cm^{-1} and is within a broader calcite feature. Another calcite feature lies between 2450 and 2650 cm^{-1}. The area of each feature was measured, an example of which is shown for location C2. Right: Peak areas of C-H and CaCO$_3$ along the transect. C-H and calcite clearly peak in or near the brown area (Figure 6).

Soil samples in the 75 µm diameter range were potted in epoxy, sectioned and polished with 1µm diamond paste. Automated particle analysis software in the SEM was used to measure size and composition, the latter using energy dispersive spectroscopy (EDS). Similar analyses were performed on loose particles. By number count, calcite particles were much more abundant in sample C (3.5%) than in sample E (0.13%). The calcite grains had a coating of clay particles (Mg-Al-SiO$_4$) adhering to their surface and the calcite appeared to be aggregates rather than detrital (Figure 7).

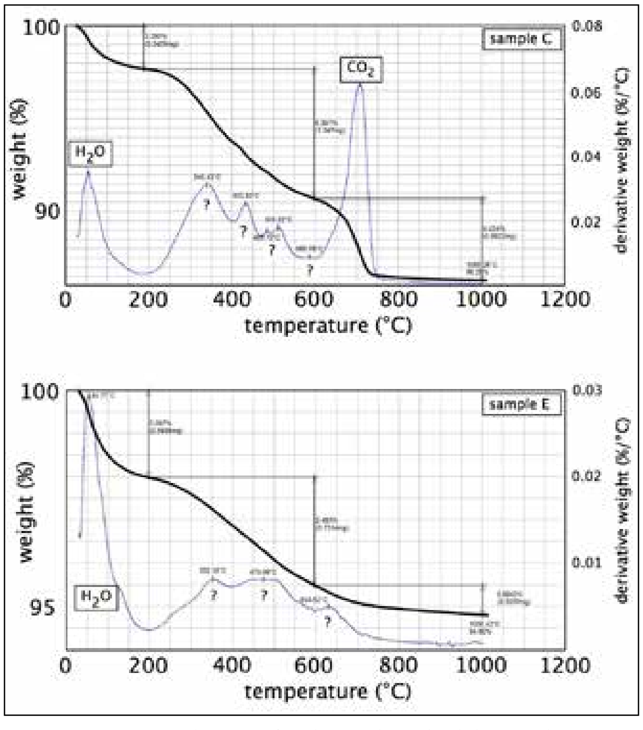

Figure 10. TGA and DTG of soil samples. Thick line is the sample weight as a function of temperature and the thin line is the negative derivative. Top: In Sample C in the brown area, the peak in the derivative at ~50C is due to evaporation of water. Near 700 °C the peak is from the release of CO$_2$ as CaCO$_3$ dissociates. Bottom: Same analysis on sample E, well outside the brown area. Note the absence of the CO$_2$ peak

Figure 8 shows ATR spectra of the soil samples normalized to the quartz peak. The CO$_3$ and H$_2$O features are well-separated, allowing relative abundance in each sample to be measured by noting height of the peak spectral features "Δ". Clearly the water and calcite are well correlated. Diffuse reflectance spectra differ from ATR spectra by having very strong H$_2$O-(OH) features between 4000 and 2300 cm^{-1}. Absorption bands from C-H and CO$_3$ are also much stronger in this region of the reflectance spectra. Figure 9 shows baseline corrected reflectance spectra between 3200-2300 cm^{-1}. C-H features occur at 2924 cm^{-1} and 2854 cm^{-1} that are in close association with calcite peaks at 2983 cm^{-1} and 2875 cm^{-1}. C-H and CaCO$_3$ are evidently well correlated. Both Figure 8 and 9 show the highest concentration of C-H, H$_2$O and CaCO$_3$ in the in the brown area at locations C and C2.

Thermogravimetric analysis (TGA) and differential thermogravimetric analysis (DTG) were performed on the soil samples. The goal was to identify chemical components of the soil and estimate the relative abundance of them. Figure 10 shows the results for samples C and E. Strong peaks in DTG of sample C in the brown area show H$_2$O evaporation and CO$_2$ release as CaCO$_3$ dissociates. When the same analysis was performed on sample E (outside the brown area), the CO$_2$ peak was absent. Based on a molar analysis of sample C, the soil was 10% calcite by weight. For sample C2 it was 12%. The source of the minor peaks between 200 °C and 700 °C is not known but in view of the large amount of plant matter, they are most likely from thermal decomposition (thermolysis) of organic material, perhaps cellulose or lignin.

6. Discussion and Interpretation

The right lateral channel offsets and sag-like depression are consistent with right-lateral slip and a slight right bend or step over in the Ivanpah fault as shown in Figure 2C and Figure 4B. Fault motion may have produced a local pull-apart basin, or "sag". Most sags collect water, and when the water evaporates, a white deposit of evaporites like halite and gypsum, are left. But this is not seen here because there is no closed basin in the vicinity of the topographic low. The depression in the profile can best be thought of as a "sag on a slope" or sidehill bench.

Enhanced vegetation is an indicator of increased soil moisture at the site. It may come from several sources: (1) tectonically crushed rock in the step-over region will open a conduit to the water table which is about few meters below the surface. Upward diffusion through the crushed rock will bring water near to the surface. (2) The speed of water (rain runoff) flowing along the surface will be lowest on the smallest slope. This occurs at the downhill part of the sag in the brown area. Thus it will spend more time in the sag and more readily percolate downward into the soil. (3) The bottom of the depression is closer to the water table than any other part of the transect, and thus one might expect enhanced vegetation. (4) Cow and burro urine will add water to the brown mantle of dung[8-10].

The depression may be fairly young, formed during the Holocene or late Pleistocene. Otherwise soil creep and aeolian deposition would have likely infilled the depression. It is also not elongated along the trace as long-lived pull-apart basins are. Slippage along the fault may have recently started and present day slippage would maintain the sag. We do not know the soil movement or deposition/erosion rate in the area, but frequent visitations by herbivores might be expected to increase the infilling of the depression. There was no seismicity in the area associated with the fault[11] based on a full search of the USGS earthquake database. It is possible the area once did contain a minimum that collected water, which would also produce enhanced vegetation, but has since been partially filled to yield its current shape.

The brown area's color is due to animal dung, probably cows and burros that we frequently encountered near the spring. Deer and Bighorn sheep are also known in the area. Optical microscopy of soils in the brown area revealed that much of the material was organic: plant stems and seed casings. Plant fiber is composed primarily of cellulose and lignin and these materials are indigestible by herbivores. As a result, they are excreted and comprise much of the dung mass. For obvious reasons, dung and urine are spatially correlated. In view of the arid climate, the only year round source of surface water would seem to be herbivore urine.

Cow and horse (burro) urine contains $CaCO_3$ in solution as bicarbonate anions and in suspension as sabulous calcite crystals[8,9]. Additionally, the amount of calcite may be increased by the biomineralization, microbiologically induced calcite precipitation (MICP)[10]. Herbivore urine contains urea (CH_4NO_2), a product of protein breakdown. Dung is also rich in protein, which eventually breaks down into urea and ammonia (NH_3). In the presence of soil moisture, urealytic bacteria produce ammonium and carbonate ions. This creates locally elevated carbonate concentrations that lead to supersaturation of soil solutions with respect to calcite. Calcite precipitates (biomineralization), thereby adding $CaCO_3$ to the soil where ever herbivores defecate and urinate. We have no direct evidence of this kind of biomineralization, so the C-H/$CaCO_3$ correlation is most simply explained by calcite particles in herbivore urine.

The scenario that we envision is this: Right lateral slip on a fault with a right hand step produced a depression (sag). Water tables usually follow surface contours, so the depression was closer to the water table than the sounding terrain. With more available soil moisture, vegetation became enhanced. This attracted cows and burrows, which deposited dung and urine in the soil. Urine added moisture to the soil so the plants grew better. Urine also carried $CaCO_3$ and nutrients to the soil like urea, phosphorus and nitrogen. Plants flourished and further attracted herbivores. Thus the system is or could become self-perpetuating as herbivores watered and fertilized the soil. Eventually the depression will be filled in by soil creep unless fault slip occurs in subsequent earthquakes.

7. Summary

The Ivanpah Spring Fault is a right lateral transform fault with a right hand step that produces a sag-like structure. The sag does not collect water because it is on a slope. Herbivores are attracted to the sag where they deposit dung and urine. Soil analyses show a strong correlation between pedogenic calcite and organic material as indicated by the presence of the C-H group. In areas surrounding the sag there is very little calcite or organic material. The C-H originates from herbivore dung and the calcite is probably deposited directly as solid particles in suspension in herbivore urine.

Acknowledgements

The authors thank Jerry Treiman and Frank Jordan for useful discussions on the tectonics of the area, and Jon Chorover for drawing our attention to chemical properties of herbivore dung and urine, and to the possibility of microbiologically induced calcite precipitation. Joann Stock, George Rossman and Elizabeth Haddon contributed many helpful comments to an early draft of this paper. We are indebted to land owner Gerald Sauer for permission to visit the site and Lauria Lynch-German for assistance in the field.

References

1. Lynch, D. K. and Paul. M. Adams, Anatomy of Ivanpah Spring, In ECSZ Does it, proceedings of the 2017 Desert Symposium, R. Reynolds (ed.), Desert Studies Center, California State University Fullerton, 288-291 (2017)
2. Vredenberg, L. http://vredenburgh.org/mining_history/pages/hensher2005-ivanpah.html (retrieved 2016, current as of Feb 2018)
3. Hewett, D.E., Geology and mineral resources of the Ivanpah Quadrangle, California and Nevada: U.S. Geological Survey Professional Paper 275, (1956)
4. Miller, David M., Surficial Geologic Map of the Ivanpah 30' x 60' Quadrangle, San Bernardino County, California, and Clark County, Nevada, U.S. Geological Survey Scientific Investigations Map 3206 (2012)
5. Wilkerson , Gregg, Comparative stratigraphy of the Clark Mountains, Mescal Range, and Ivanpah Mountains, San Bernardio County,California (http://vredenburgh.org/gw/pdf/DS2016/Report_Stratigraphy.pdf)
6. Gudmundsson, A., Active fault zones and groundwater flow, Geophys. Res. Let., 27 (18) 2993-2996 (2000)
7. APU (Advanced Photo Utility) © David S.P. Dearborn. APU was written for archaeologists who were interested in the location of sunrise and sunset points on the horizon and to identify stars in night time photographs. CHITO is a down-looking version of APU.
8. Diaz-Espineira M., Escolar E., Bellanato J, Medina J. A., Crystalline composition of equine urinary sabulous deposits. Scanning Microsc. 9(4):1071-9. (1995)
9. Finco, Delmar, Kidney Function, in Clinical Biochemistry of Domestic Animals (5th edition), eds Jiro J. Kaneko, John W. Harvey, Michael Bruss, Academic Press, 441 - 484 (1997)
10. Mortensen, B.M.; Haber, M.J.; DeJong, J.T.; Caslake, L.F. Nelson (2011). Effects of environmental factors on microbial induced calcium carbonate precipitation. *Journal of Applied Microbiology*. **111** (2): 338-349 (2011).
11. https://earthquake.usgs.gov/earthquakes/search/

20 Feb 2018